Pergamon

PII: S0038-092X(98)00065-6

Solar Energy Vol. 63, No. 3, pp. 135–146, 1998

0038-092X/98 $—see front matter

DETERMINATION OF ATMOSPHERIC TURBIDITY FROM THE DIFFUSE-BEAM BROADBAND IRRADIANCE RATIO

C. GUEYMARD*,‡,§ and F. VIGNOLA**,‡
* Florida Solar Energy Center, 1679 Clearlake Road, Cocoa, FL 32922-5703, U.S.A.
** Physics Department, University of Oregon, Eugene, OR 97403-1274, U.S.A.

Received 12 January 1998; revised version accepted 12 June 1998

Communicated by RICHARD PEREZ

Abstract—A semi-physical method is proposed to evaluate turbidity from broadband irradiance measurements and other atmospheric parameters. This method demonstrates the utility of diffuse data when estimating atmospheric composition with broadband irradiance data. An error analysis and various tests against measured data show that this method can predict accurate turbidities provided that the sky is perfectly cloudless and the diffuse irradiance data are very accurate. Yet, this method is insensitive to errors in input data such as precipitable water and ozone amount. Applications of this method to the quality control of radiation data are discussed. Tests with actual data from Florida and Oregon show good agreement with other methods. Evaluation of the model required a detailed discussion of the accuracy and cosine error of pyranometers, and the uncertainty in precipitable water estimates. © 1998 Elsevier Science Ltd. All rights reserved.

1. INTRODUCTION

Accurate determinations of turbidity normally require clear-sky spectral radiation data obtained with sunphotometers or spectroradiometers. As these instruments are expensive and scarce, turbidity is generally estimated instead from *broadband* irradiance measurements. In recent years, most investigators have been using direct beam irradiance measured with an unfiltered pyrheliometer to obtain turbidity (e.g. Al-Jamal *et al.*, 1987; Cañada *et al.*, 1993; Fox, 1994; Freund, 1983; Grenier *et al.*, 1995; Gueymard, 1998; Gueymard and Garrison, 1998; Kambezidis *et al.*, 1993; Louche *et al.*, 1987; Maxwell *et al.*, 1995; Polavarapu, 1978; Rawlins and Armstrong, 1985; Uboegbulam and Davies, 1983). However, to obtain the aerosol transmittance or optical depth with just beam irradiance, all other atmospheric extinction processes need to be known *a priori*. This may become a problem when the water vapor and ozone columns are not continuously measured onsite, as is generally the case. In particular, important short-term errors on precipitable water may result from the usual estimation method based on surface data of temperature and humidity. Errors in the precipitable water vapor are inversely reflected in the predicted turbidity values using this beam irradiance approach (Gueymard, 1998). It will be shown that one important advantage of the present irradiance ratio method is that this method maintains its accuracy even when uncertainties in precipitable water estimates are high.

At the spectral level, it has been shown by O'Neill *et al.* (1989) that the aerosol optical depth could be retrieved from the ratio of global to direct irradiance as effectively as it is from direct irradiance only. A similar approach, but one using the ratios of *broadband* diffuse and beam irradiance, is investigated here. The potential advantage of this method is that it is less sensitive to the influence of ozone and water vapor, because these constituents deplete the beam and diffuse spectrum almost equally (Herman *et al.*, 1975). Drawbacks of this method, however, are that it is more sensitive to instrumental error because two radiometers are involved (instead of one) and that it is dependent on additional factors such as ground albedo and aerosol optical properties. This *preliminary* contribution is aimed at delineating the relative merits and limitations of this method compared to others, and at suggesting some useful applications. The methodology used to derive the model is first presented in Section 2. An error analysis of the method is described in Section 3, followed by detailed experimental comparisons in Section 4. This article presents a proof of concept. Further work is necessary

‡ISES member.
§Present address: 2959 Ragis Road, Edgewater, FL 32132-2905, U.S.A.

to expand it and test it under a greater variety of aerosol climatologies.

2. METHODOLOGY AND MODEL

The *diffuse-beam ratio model* is developed using an approach that is similar to the *beam irradiance method* used to obtain broadband aerosol turbidity from just direct irradiance (Gueymard, 1998). Clear-sky spectral irradiances are estimated using the SMARTS2 spectral radiative code (Gueymard, 1994b; Gueymard, 1995) that was also used for the beam irradiance method. Modeled spectral irradiances are summed over the range of wavelengths sensed by the two types of broadband radiometers used to make the measurements. For comparisons with direct beam irradiance, the spectral irradiance is summed from 0.28 to 4 μm. For comparisons with diffuse or global measurements, the spectral irradiance is summed from 0.28 to 2.8 μm.

A preliminary series of parametric runs is performed so that the predictions of direct, diffuse and global irradiances can be related to turbidity. It is then possible to reverse the method and obtain turbidity from measured irradiance data. The parametric runs cover a large range of atmospheric variables: zenith angle ($Z=0$–88°), pressure ($p=600$–1020 mbar), precipitable water ($w=0$–6 cm), ozone amount ($u_o=0$–0.5 atm-cm) and aerosol turbidity (expressed here in terms of Ångström's β coefficient and varied in the range 0–0.4).

To facilitate model development, a fixed *continental aerosol* model is considered here (IAMAP, 1986) for which the spectrally averaged wavelength exponent α is 1.14 over the whole spectrum, and more particularly 1.335 between 0.5 and 4 μm. It is thus close to the conventional value of 1.3 that has been used in virtually all broadband turbidity models since the pioneering work of Ångström. Other aerosol models would produce different irradiances, even for a given turbidity. This is due to the fact that the extinction processes in an aerosol layer are governed by the latter's detailed spectral properties, such as optical depth, single-scattering albedo and asymmetry factor. However, these characteristics can change significantly with time and location and are not usually known *a priori*. Therefore, some simplifying assumptions are necessary to allow generalization to the majority of cases. In the present case, the chosen continental aerosol model should be typical of locations away from any predominant influence of maritime, urban or desert aerosols. A continental aerosol model with an α value close to 1.3 is used here because no better value can be obtained at any instant without specialized instrumentation. Moreover, this simplifying assumption is the most practical one when dealing with broadband data because it corresponds to the climatological average value of α at most sites, and is thus typical for most cases. This assumption has been used extensively in the literature (e.g. Barbaro *et al.*, 1989; Cañada *et al.*, 1993; Gueymard, 1998; Jacovides *et al.*, 1994; Katsoulis, 1979). Small variations of α around the 1.3 value have little effect on β. Additional calculations with SMARTS2 have shown that a variation of 0.1 around $\alpha=1.14$ produced an opposite variation of about 3% in β. If maritime aerosols are simulated, with a typical average α value of only 0.27, they produce β values about 30% larger than with the present continental model, for otherwise identical conditions.

Although turbidity is expressed here in terms of Ångström's coefficient β only, other coefficients (such as those proposed by Linke, Schüepp and Unsworth–Monteith) could be used alternatively. Their relationship with β is detailed in a previous paper (Gueymard, 1998).

When beam irradiance is measured, it is often accompanied by simultaneous measurements of global and/or diffuse irradiance. This contribution presents a study on how to make use of this added information. The fundamental relationship between the beam, global and diffuse radiation components is

$$E=E_{bn}\cos Z+E_d=E_b+E_d \qquad (1)$$

where E, E_b and E_d are the global, direct and diffuse irradiances on a horizontal surface, respectively, E_{bn} is the direct beam normal irradiance, and Z is the sun's zenith angle. It should be noted that all irradiance calculations performed here include a correction for the circumsolar radiation that is included within the aperture cone of pyrheliometers (typically, 3° around the sun's center). Assuming the circumsolar radiation is symmetrically distributed around the sun, the circumsolar radiation can be projected onto the horizontal surface by the $\cos Z$ factor just like beam irradiance.

According to eqn (1), any irradiance ratio, such as E_d/E, E_d/E_{bn} or E_b/E_d, can be expressed in terms of any other one and Z. Selecting any one of these irradiance ratios to estimate turbid-

ity appears arbitrary because of their mathematical interdependence, although only a few such ratios have been investigated so far. A literature survey shows that only the ratios $K=E_d/E$ (e.g. Dogniaux and Doyen, 1968; Jacovides *et al.*, 1995; Unsworth and Monteith, 1972), $K_{bg}=E_b/E$ (Pinazo *et al.*, 1995) and $K_{db}=E_d/E_{bn}$ (Gueymard, 1989; Wesely and Lipschutz, 1976) have been purposely used as an indirect measure of turbidity. The effect of turbidity on K and K_{db} is shown in Figs 1 and 2, respectively. It clearly appears that K_{db} is preferable because it varies almost linearly with β, and varies little with Z, especially for $Z\leq 75^\circ$. (This pseudo-linearity in turbidity can also be observed in the results shown by King and Herman (1979) for spectral radiation at 0.555 μm.) This finding has proven to be of considerable importance to obtain an accurate fit in β and Z. The other ratios tested, namely E_b/E_d and E_b/E, were found to have the same kind of behavior as K and could not be fitted with sufficient accuracy. The linear behavior of K_{db} and its relative insensitivity to Z appear to be retained for a large range of atmospheric conditions. Consequently, K_{db} should be relatively constant over a day if turbidity does not vary, as has been noticed before (Weber and Baker, 1982).

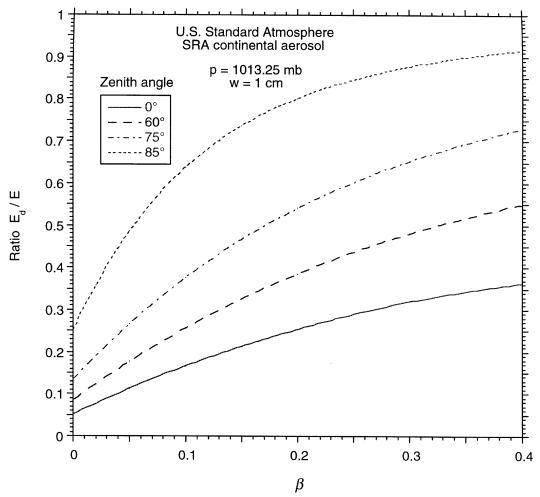

Fig. 1. Irradiance ratio $K=E_d/E$ as a function of β and Z.

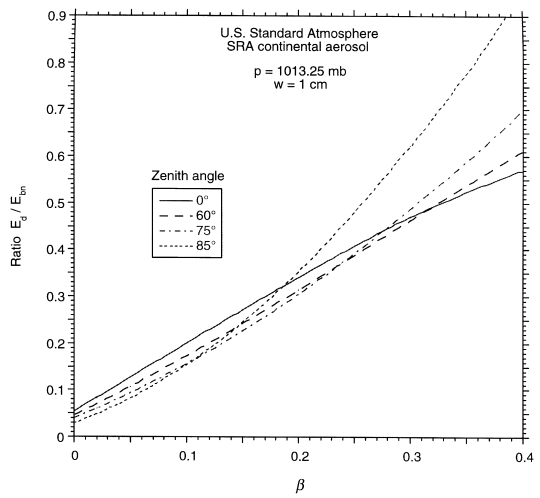

Fig. 2. Irradiance ratio $K_{db}=E_d/E_{bn}$ as a function of β and Z.

From the large number of parametric runs performed with SMARTS2, it has been found that K_{db} can be accurately parameterized as

$$K_{db}=(a_0+a_1\beta+a_2\beta^2)/(1+a_3\beta^2) \qquad (2)$$

where the coefficients a_i are themselves functions of Z, p, u_o and w, as detailed in Appendix A. Note that the functional form of eqn (2) guarantees a proper fit for any Z and any $\beta\leq 0.4$, even outside of the linearity zone mentioned above. If an experimental value of K_{db} is obtained from measurements, eqn (2) can be easily solved to obtain β as follows

$$\beta=0.5\{[a_1^2-4(a_2-a_3K_{db})(a_0-K_{db})]^{0.5} -a_1\}/(a_2-a_3K_{db}). \qquad (3)$$

A correction needs to be applied if the average ground albedo, ρ_g, of the measurement site's area is not equal to the reference value used here, 0.15. This correction results from back-scattering processes between the ground and the sky of albedo ρ_s. The latter has been fitted as a function of β from parametric runs of SMARTS2

$$\rho_s=(0.065974+0.77161\beta)/(1+1.4881\beta). \qquad (4)$$

The limit value of ρ_s calculated from eqn (4) for $\beta=0$, the case of an ideally aerosol-free (or "Rayleigh") atmosphere, is close to the value of 0.0685 obtained by Lacis and Hansen (1974).

The rapid increase of ρ_s with β is such that the global irradiance for both a highly reflective ground and a hazy sky can be significantly larger than the irradiance for the reference case ($\rho_g=0.15$). The irradiance for the general case, $E(\rho_g)$, is related to the reference irradiance, $E(0.15)$, through

$$E(\rho_g)/E(0.15)=(1-0.15\rho_s)/(1-\rho_g\rho_s). \qquad (5)$$

As ρ_s depends on β, which is the unknown, eqn (5) needs to be solved iteratively along with Eqns (3) and (4).

3. COSINE CORRECTION AND ERROR ANALYSIS

As with all models, there is a limit to the accuracy to which one can determine the sought-after results. This section discusses the sources of uncertainty of the method, as well as their magnitude. A way to improve the accuracy of the measured global irradiance is also proposed through proper correction of the pyranometer's cosine response.

First, the accuracy of the SMARTS2 model is analyzed in comparison to more rigorous spectral models. Next, the sensitivity of the modeled results to the accuracy of measurement is described. Finally, the effects of the cosine error of pyranometers are examined along with their effects on the determination of β. (The accuracy of the global radiation data are the limiting factor in the analysis of the irradiance ratio method since this study is based on diffuse data obtained by subtracting the direct component from global measurements. The departure from true cosine response is the largest source of error in global measurements.)

Comparisons between the modeled K_{db} and reference calculations obtained with Monte-Carlo and spherical harmonics rigorous codes (Bird and Hulstrom, 1982; Braslau and Dave, 1973), show good to excellent agreement, with an uncertainty estimated to be 5%. This includes the fitting error embedded in eqn (2), which is less than 1%. From Fig. 2, an approximate expression for K_{db} when $\beta<0.35$ and $Z\leq 75^\circ$ would be

$$K_{db}=0.04+1.45\beta. \quad (6)$$

After differentiation, this gives

$$\Delta\beta/\beta=(1+0.0276\beta^{-1})\Delta K_{db}/K_{db}. \quad (7)$$

Therefore, a variation of 5% for the modeled K_{db} would translate into moderate errors in β of from 6% for a hazy sky ($\beta\approx 0.2$) to 12% for a very clear sky ($\beta\approx 0.02$).

Experimental errors play a significant role in limiting the accuracy to which β can be estimated. The error in E_{bn} may be low (typically $\pm 2\%$) if a regularly checked and calibrated temperature-corrected pyrheliometer is used. (Egregious errors resulting from mistracking are not considered here.) The error in E_d may be far larger because diffuse radiation cannot be easily measured. Frequently the monitoring station consists of a single-pyranometer/pyrheliometer combination and E_d is calculated using eqn (1). Under very clear skies, E and E_{bn} are two large numbers resulting in a small E_d. As an example for $Z=30^\circ$, $\beta=0.02$, $w=1$ cm and $u_o=0.3$ cm, SMARTS2 calculates $E_{bn}=1012$ W m^{-2}, $E=958$ W m^{-2} and $E_d=81$ W m^{-2}. If the measurement of E was off by -5% (a typical value for field conditions (Myers *et al.*, 1989)) this would lead to an error of -60% in E_d calculated using eqn (1). In this case, an error of -60% in E_d would translate directly into a -60% error in K_{db}. The resulting β would be *negative*. Therefore, good quality turbidity estimates from the irradiance ratio method require extremely accurate global and/or diffuse measurements.

A special setup is now used at some first class experimental sites, like those of the BSRN/WMO network, to achieve high accuracy in both diffuse and global radiation measurements. It consists in measuring direct beam radiation conventionally with a pyrheliometer (preferably of an active cavity type) and adding diffuse radiation measured with a pyranometer/tracking shade apparatus to indirectly obtain global radiation, i.e. the reverse procedure to what was described above. A noticeable gain of accuracy, particularly under clear skies, has been reported recently with this new procedure (Michalsky and Dutton, 1997; Michalsky *et al.*, 1998). Such a setup simply eliminates the need for cosine error correction in the global radiation data that is now described.

An important source of the measurement error in pyranometers comes from their cosine error, i.e. their deviation from true cosine response as the angle of incidence changes. Recent laboratory measurements (Michalsky *et al.*, 1995) have shown that this error is non-negligible, and may also be compounded by azimuth and other errors. Each pyranometer should be individually characterized so that its cosine/azimuth error can be compensated during the quality control process. However, measurement of the cosine and azimuth errors is not precise and the size of the errors changes over time. In practice, the measurement of these errors is very time-consuming and expensive to obtain. Generally such manipulation of the data is not implemented because of the possibility of introducing systematic errors into the data and the inability to check on the accuracy of the changes made.

Because the irradiance ratio method is so sensitive to the diffuse value, the cosine error shows up clearly in the broadband turbidity data analysis. Since measurements of the cosine

errors are generally not available, it is necessary to correct the pyranometric data by use of a *generic* cosine error typical of the type of instrument used. An example is given here for the Eppley PSP that is widely used in the U.S.A. and elsewhere. Laboratory data for the instrument response at various incidence angles (0–88°) have been used here (Michalsky *et al.*, 1995). This dataset contains results from three individual pyranometers and indicates a "remarkable reproducibility" (Michalsky *et al.*, 1995), so that the analysis presented here is of general validity for this particular type of instrument, with an assumed minimal instrument-to-instrument variance. The cosine response for each instrument was originally measured along two opposite bearings, or azimuths, on the optical bench. The resulting asymmetry is insignificant, so that the azimuthal effect in this case can be eliminated by taking an average of the cosine response at these two azimuths. The average *normalized cosine response*, C_b, thus obtained for these three instruments and two azimuths is shown in Fig. 3. By definition, this factor is the ratio of the instrument response to that of a perfect cosine receptor, normalized to 1 at normal incidence. These data points have been fitted with

$$C_b = (1 - 0.010987\theta - 9.8179\mathrm{E}-6 \times \theta^2 + 9.6321\mathrm{E}-8 \times \theta^3)/(1 - 0.010979\theta) \quad (8)$$

where θ is the incidence angle (equal to Z for a horizontal instrument). For ideally isotropic diffuse illumination, the average factor for diffuse radiation would be

$$C_d = \int_0^{90} C_b(\theta) \sin 2\theta \, d\theta \Big/ \int_0^{90} \sin 2\theta \, d\theta \quad (9)$$

or $C_d = 0.96706$ after numerical integration. This value corresponds to an effective incidence angle $\theta_e = 51.4°$ in eqn (8).

The practical use of C_b and C_d depends on the calibration process for each pyranometer. For pyranometers calibrated with the outdoor shading/unshading method at *normal incidence*, such as practised at the Florida Solar Energy Center (FSEC), the corrected direct and diffuse irradiances, which need to be added to obtain the corrected global irradiance, would be $E_b = E_{bx}/C_b$ and $E_d = E_{dx}/C_d$, respectively, where E_{bx} and E_{dx} are the experimental, uncorrected components, which combine onto the pyranometer sensor to give the experimentally measured global irradiance, E_x. For instruments calibrated in a fixed *horizontal* position, such as practised at the National Renewable Energy Laboratory (NREL), the calibration factor integrates the effect of C_b to a certain extent, depending on the *average* Z at which the calibration is made. For Z limited to 45–55°, as followed at NREL, the corrected irradiances would be $E_b = C_b(50°)E_{bx}/C_b(Z)$ and $E_d = C_b(50°)E_{dx}/C_d$. Finally, for an indoor calibration performed inside a white chamber under isotropic diffuse radiation, as followed by Eppley and some national networks (Latimer, 1972), the corrected irradiances would be $E_b = C_d E_{bx}/C_b$ and $E_d = E_{dx}$.

This correction method is not perfect because it does not take into account the unavoidable instrument-to-instrument differences. Azimuthal errors could be modeled because some laboratory data are available, but the exact azimuthal bearing of a field pyranometer is generally not known or accessible to the data user. However, it is clear from the earlier discussion on the sensitivity of the irradiance ratio method to accurate diffuse data and the size of the cosine error shown in Fig. 3 that compensation of the cosine error is necessary, particularly at large zenith angles where large cosine errors may occur.

Recently, diffuse data made with tracking shade disks is becoming available. As mentioned earlier, such diffuse data would be a much more accurate measurement of the diffuse values and eliminate much of the concern about cosine errors.

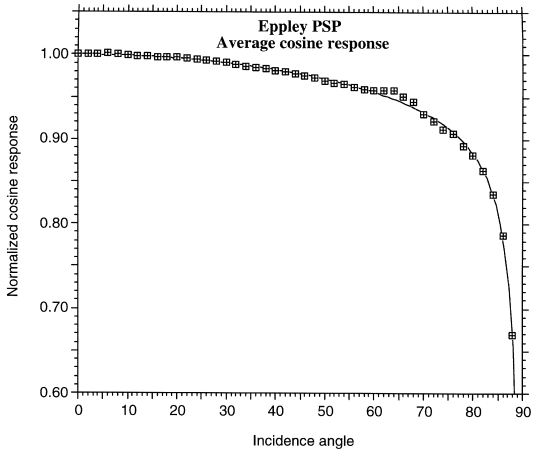

Fig. 3. Normalized cosine response of the Eppley PSP pyranometer, from laboratory data.

4. EXPERIMENTAL COMPARISONS

In addition to the error analysis above, experimental verification of the model is needed to test its ability to predict the correct turbidity under non-ideal atmospheric conditions. Limited experimental comparisons are presented to validate the concepts. More experimental spectral data are being collected from different sunphotometric networks and further tests will be offered in a subsequent contribution. In particular, new instrumentation (pyranometer/tracking shade for diffuse irradiance and multifilter rotating shade radiometer for spectral aerosol optical depth) is being added at the University of Oregon radiation site which will soon permit a detailed performance assessment.

The initial comparison was conducted with data measured at FSEC, Cape Canaveral, FL (lat. 28.42°N, long. 80.61°W, alt. 7 m). A hazy and humid summer day is selected here first to test the performance of the present model under turbid conditions. This particular day was selected previously (Gueymard, 1998) to test the beam irradiance method (where β is derived from E_{bn} only) against an independent determination of β derived from spectroradiometric data. Precipitable water was calculated from 5-min ground observations of air and dew-point temperature using an empirical relationship (Gueymard, 1994a), and was roughly constant at about 5 cm for the day. This is in agreement with radiosonde data from the nearby Kennedy Space Center. Broadband observations of E_{bn} and E were available at 5-min intervals also. These measurements are used here to derive β from the beam irradiance model (Gueymard, 1998) and from the present diffuse-beam ratio method (or K_{db} model). The latter model is used with and without cosine correction of the global irradiance data (E) in accordance with the discussion in Section 3.

There is excellent agreement between the different methods, especially when the cosine correction is applied to the data. Between 6:30 and 8:30 LST, when the sky was hazy but cloud-free (Fig. 4), the agreement is excellent. The rapidly decreasing turbidity between sunrise and 6:30 was caused by a dissipating fog, a frequent occurrence in this area due to the very high humidity. After 8:30, cloudiness began to build up (very thin or subvisual cirrus at first), resulting in an obscured sun after 11:00 until sunset. For the particular conditions of this test, ignoring the cosine correction results in an underestimation of about 3–6% in β, in accordance with the error analysis in Section 3.

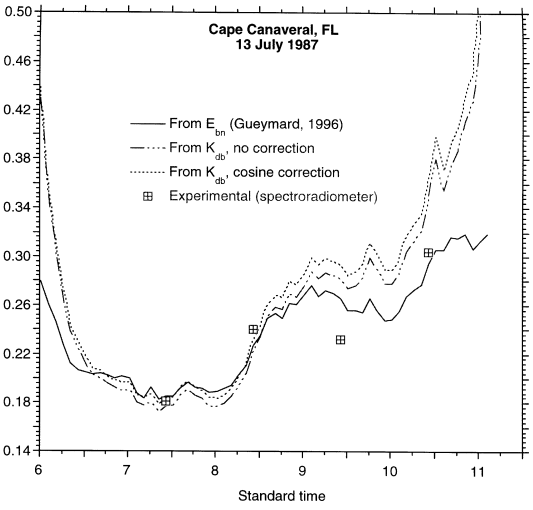

Fig. 4. Experimental comparison of the present method to results obtained with that of the beam irradiance method of Gueymard (1998) for a hazy summer day at Cape Canaveral, FL.

A similar comparison at FSEC is shown for an exceptionally clear summer day in Fig. 5. Some fog was again present between sunrise and 6:30, but then the rest of the day was essentially cloud-free, except for a few non-obscuring clouds between 7:30 and 10:00. The predicted β showed a remarkable stability at about 0.06 during the whole day, with good to excellent agreement between the different methods to obtain β.

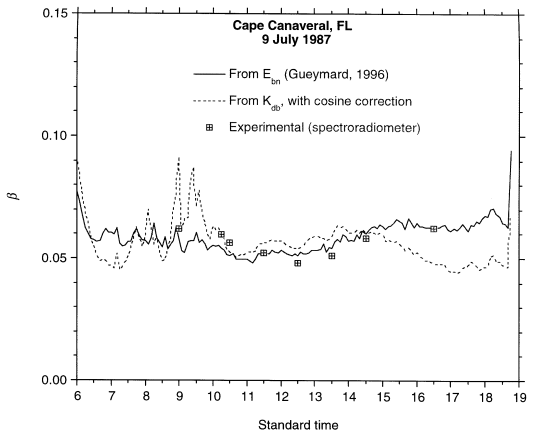

Fig. 5. Experimental comparison of the present method to results obtained with that of the beam irradiance method of Gueymard (1998) for a clear summer day at Cape Canaveral, FL.

As could be expected, the present method is more sensitive to partial cloudiness than that of the beam irradiance model (Gueymard, 1998), which needs only a clear line of sight in a 5° cone around the sun's center. Because clouds absorb and scatter radiation more than aerosols, and thus have a profound effect on E_d, the ratio K_{db} is very sensitive to the presence of clouds in the sky, even if they do not obscure the sun. Hence the progress of the mismatch between the two broadband methods before 6:30 and after 8:30 in Fig. 4, or between 7:30 and 10:00 in Fig. 5. This finding has two important consequences. First, the diffuse-beam ratio method is valid only for truly *cloud-free* atmospheres, thus restricting its use compared to methods based on E_{bn} alone. Second, this limitation may become a strength if the diffuse-beam ratio method is used not to obtain β, as originally intended, but to detect cloud-free conditions in real-time or historic data. This may prove to be an important application because it is always very difficult to select clear conditions *a posteriori*, from radiative data alone.

In Fig. 5, the difference between the two methods of calculating β from 15:00 to sunset is on the order of 20–30%. Uncertainties in the global measurements can account for most of this difference. Measurement of the diffuse radiation with a tracking disk would eliminate most of this uncertainty and provide for a much more stringent test of the model.

For general applicability of the irradiance ratio method, estimates of β need to be compared on a variety of conditions. Insolation data measured at Miami, FL (lat. 25.78°N, long. 80.27°W, alt. 2 m) and included in the National Solar Radiation Data Base (NSRDB) of NREL are used for the basis of the long-term comparison. Hourly cloud observations and meteorological data from Miami airport are also available in the NSRDB. The test period was chosen here as 1978–1980 because irradiance data were then of good quality (Maxwell *et al.*, 1995). For this site, as well as the other sites below, no direct observation of turbidity based on spectral data were available, so that the present ratio method could be only assessed by comparison with the beam irradiance method of Gueymard (1998), chosen here as the reference. In all what follows, potentially cloud-free periods at the radiation site are assumed if the observed hourly cloud cover is less than one-tenth. The resulting turbidity estimates are also checked for consistency. Because the optical depth of clouds is at least one order of magnitude greater than that of aerosols (e.g. about 2 for a cirrus), their inadvertent passage in front of the sun during even a small fraction of a supposedly clear hour results in a very high apparent turbidity. Consequently, all spikes in hourly turbidity during the day are interpreted here as cloud interference and subsequently removed from the dataset. Figure 6 indicates a reasonably good match between the two predictions of β at least for low to medium turbidity ($\beta < 0.15$). The progressive mismatch which is apparent above this threshold may have different causes. A very probable cause is the interference due to undetected passages of non-obscuring clouds, which affect the present method more than the reference method. Of course, another explanation is that the model itself needs to be refined for days with a high turbidity factor. In particular, the progressive mismatch might be due to the unsuitableness of the simplifying assumptions in Section 2 under hazy skies.

A third series of examples come from data measured at Eugene (lat. 44.047°N, long. 123.071°W, alt. 150 m) and Burns (lat. 43.87°N, long. 119.03°W, alt. 1265 m), OR. These two stations are maintained by the University of Oregon (UO). Their radiometric setup is identical to that at FSEC, except that the UO's pyranometers are calibrated at NOAA Boulder, CO, by side-by-side intercomparison with a reference instrument. Besides the 5-min radiometric data from the Eugene station, cloud cover and other meteorological data are available from each city's airport.

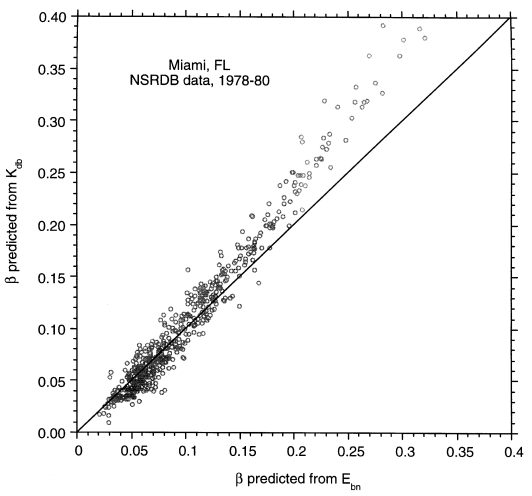

Fig. 6. Experimental comparison of β obtained with the present method to that obtained with the beam irradiance method of Gueymard (1998) for hourly clear periods at Miami, FL.

Figure 7 represents a clear summer day at Burns, using only input hourly data from the NSRDB. (The Burns and Eugene *radiation* data in the NSRDB come from the UO Solar Radiation Monitoring Network.) This day is of particular interest because of the transition in turbidity that occurred from the relatively low value that was prevalent during the preceding days ($\beta = 0.02$–0.06) to a relatively high value which continued for two more days ($\beta = 0.12$). In the absence of radiosonde data to obtain precipitable water directly at Burns, it was predicted by an empirical method (Gueymard, 1994a) from surface temperature and humidity. In the upper plot of Fig. 7, the hourly values of w thus obtained are compared to the NSRDB values, taken directly from the hourly file. This comparison shows relatively poor agreement and the need for better data and models for determining water vapor. The accuracy of the precipitable water is very important for the beam irradiance method because if precipitable water is *under*estimated, the turbidity predicted from E_{bn} will be *over*estimated, and vice versa. This problem was pinpointed in previous contributions (Gueymard, 1998; Gueymard and Garrison, 1998). In Fig. 7, the use of the NSRDB precipitable water values would considerably lower the turbidity values shown for the E_{bn} model.

In attempting to evaluate the NSRDB precipitable water values, the authors determined that there was a misprinted coefficient in the original publications (Maxwell *et al.*, 1995; Myers and Maxwell, 1992). This was later confirmed by the developers of the NSRDB (personal communications with Gene Maxwell and Steve Wilcox, NREL, 1997).

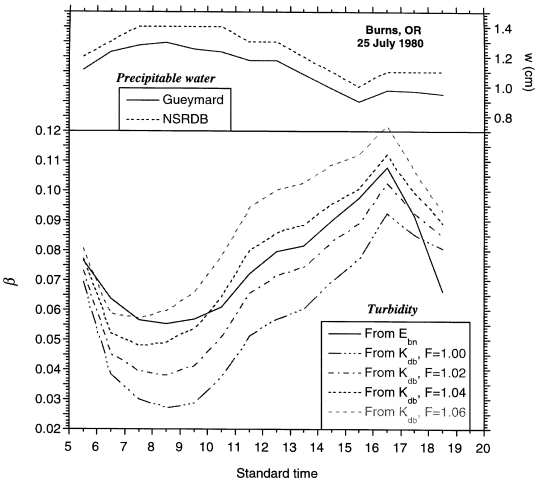

Fig. 7. Hourly turbidity and precipitable water for a clear summer day at Burns, OR.

Figure 7 also shows that no overall match is found between the value of β predicted from E_{bn} and that predicted from K_{db}, even when considering the cosine error correction. The same pattern reproduced systematically during other clear days, with an abnormally large number of unphysical (negative or near-zero) turbidity predictions with the K_{db} method. For all the thousands of clear periods examined (using either 5-min or hourly irradiances), the only way to force a match between the two predictions of β was by multiplying the cosine-corrected experimental value of global irradiance by a constant correction factor, F. Calculations were repeated for different arbitrary values of F, as shown in Fig. 7. This series of simulations for different F values provides a sensitivity analysis of the method with respect to the overall uncertainty in the measured global irradiance, partly due to the cosine error discussed earlier. A good match could then be obtained for the case of Fig. 7 with $F = 1.035$. The same pattern was prevalent throughout 1980, and a yearly average value of 1.046 was found. This problem also appeared in 1988—the other test year chosen here—but with a lower average value, $F = 1.005$. The magnitude of this correction and its abrupt change between 1980 and 1988 is consistent with the fact that NREL, during the production of its NSRDB, *a posteriori* increased the global irradiance data measured at Burns by 6% from November 1985, thus signaling a calibration problem. All this suggests that the present method is very sensitive to the accuracy of the global irradiance measurements. Conversely, it has also some useful potential in data quality control because even slight miscalibration of pyranometers appears to be easily detectable *a posteriori.* All this is based on many assumptions that need verification, including that continental aerosols are prevalent above the high desert plateau in eastern Oregon where Burns is located.

Because of the uncertainty in precipitable water predictions mentioned earlier, it is important to investigate the effect it may have on β predictions from either E_{bn} or K_{db}. A particular case is illustrated in Fig. 8 for a clear day in Eugene. (The early morning spike is due to an obstruction greatly affecting E_{bn}.) For that day, morning predictions of w using the airport data of temperature and relative humidity agreed relatively well with those obtained from the same type of measurement performed at the

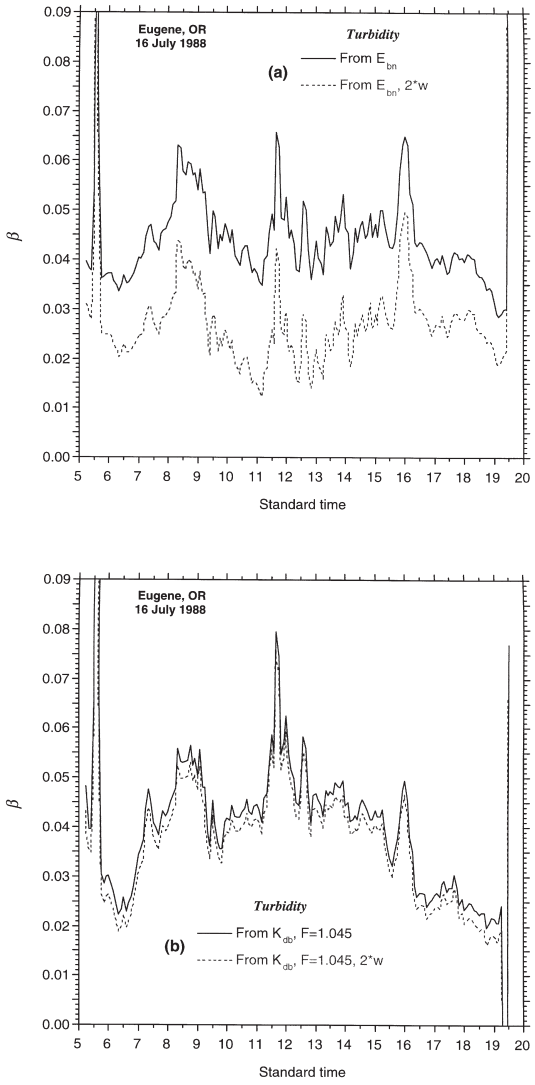

Fig. 8. Effect of doubling precipitable water on turbidity predictions for a clear summer day at Eugene, OR. (a) Using the beam irradiance method of Gueymard (1998); (b) using the diffuse-beam ratio method (this work).

UO's radiometric station. A marked drop in the UO's w occurred after 14:00 LST, leading to values less than *half* those obtained with the airport data between 15:00 and 18:00. Such a large discrepancy in w is not exceptional, and it is not clear if it corresponds to a real difference due to horizontal inhomogeneities in w or to some instrumental problem, but the latter explanation is more likely. Predictions of β were thus done with either the UO's predicted w at 5-min intervals, or with twice this value. A constant correction factor, $F=1.045$, was also used. As can be seen from Fig. 8, doubling precipitable water has a profound effect (a 50% decrease) on β predicted from E_{bn}, but only a negligible effect (2–4% decrease) when predicted from K_{db}. Also, it can be observed from Fig. 8 that a good match between the two turbidity methods is obtained until 15:30, when β was calculated from E_{bn} with w. After 15:30, the models using twice w tend to agree. Another explanation is that the zenith angle starts to drop rapidly in the afternoon and departures from the modeled cosine correction factor could also account for a part of the discrepancy.

These findings confirm that the present ratio method is preferable to the beam irradiance method when the accuracy of precipitable water data is uncertain. However, further research is needed to characterize the range of climatic conditions under which one method is preferable to the other.

5. USE OF THE IRRADIANCE RATIO METHOD TO ASSESS GLOBAL DATA

Because the diffuse-beam ratio method is so sensitive to the accuracy of global and diffuse irradiance data, it may be possible to use the model to assess the quality of the global data. Figure 7 showed one way of using the irradiance ratio method to test the accuracy of global irradiance measurement, but this implied iterations to obtain the precise value of F needed to correct E. A simpler way consists in using β predicted from E_{bn} (Gueymard, 1998), then calculating K_{db} from eqn (2). Hence a predicted value of E can be obtained from $E_{\mathrm{bn}}(\cos Z + K_{\mathrm{db}})$. This value of E can be ratioed to its measured, cosine-corrected counterpart to obtain F. It can also provide a good estimate for E whenever the measured global irradiance is either unavailable or questionable. Preliminary tests indicate that a very high accuracy in E is achievable with this method. This is illustrated for Burns and Eugene in Fig. 9Fig. 10, respectively. Hourly NSRDB data for one year (1988) were used in both cases. A very high correlation coefficient ($R>0.999$) of the least-squares fits between each pair of global irradiance sets (predicted vs measured) is obtained, as well as a remarkably low scatter. The fitted values of F thus obtained for 1988 are 1.0046 at Burns and 1.0447 at Eugene. A slight downward curvature is noticeable in these plots. The use of non-cosine-corrected data significantly increases this curvature. This suggests that the cosine correction used here effectively improves the method, although it is probably not fully optimized yet.

The interest of using this method in quality

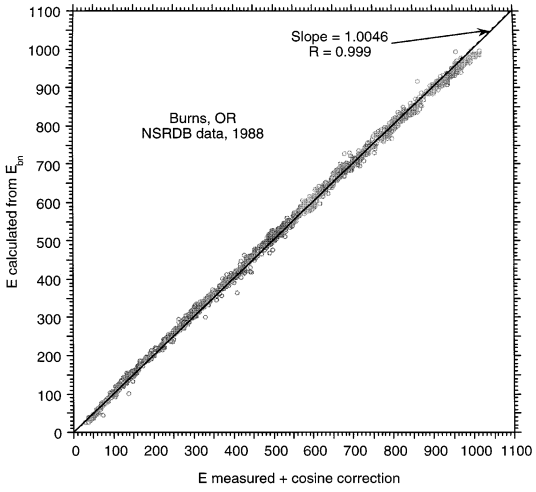

Fig. 9. Experimental comparison of the global irradiance predicted by a combination of the beam irradiance method of Gueymard (1998) and the present method for hourly clear periods at Burns, OR.

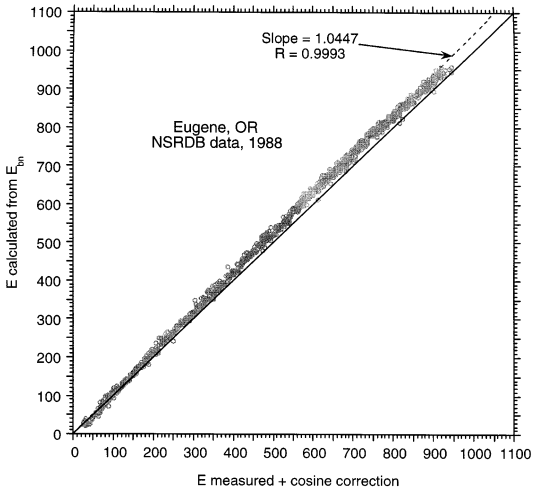

Fig. 10. Experimental comparison of the global irradiance predicted by a combination of the beam irradiance method of Gueymard (1998) and the present method for hourly clear periods at Eugene, OR.

control processes (e.g. testing for the correct calibration constant of pyranometers or its drift with time) will be investigated further in a separate study.

6. CONCLUSION

A semi-physical method for turbidity determination from broadband irradiances has been presented and partially validated. This method requires cloudless skies and very accurate measurements of global (or diffuse) and direct radiation. These conditions appear very restrictive compared to more conventional turbidity methods based on direct irradiance only. However, the diffuse-beam ratio model has the advantage that it is far less dependent on atmospheric ozone and, even more importantly, on precipitable water, which can be very difficult to estimate on an hourly basis. Thus, the diffuse-beam ratio method should be preferred over the beam irradiance method whenever precipitable water cannot be estimated with good accuracy.

There are many potential uses for this new procedure because of the method's sensitivity to measured diffuse irradiance and its insensitivity to exact values of water vapor and atmospheric ozone.

(1) Comparison of the beam and diffuse-beam ratio model results can narrow the range of acceptable water vapor estimates when accurate diffuse data are available.
(2) Comparison of the two methods can help identify truly cloudless periods in the historical record.
(3) Comparison of the two methods can be used to examine the deviation from true cosine response of pyranometers.
(4) Combination of the two methods can be used to estimate global insolation. This process can be used to generate global data (from direct beam data) when none is available or to quality assess the global data when it is available.

This model demonstrates one method to extract useful information from the diffuse component. As more accurate data becomes available for testing and refining the model, the utility of the model and confidence in its applications will improve.

Acknowledgements—We are thankful to Dr Joe Michalsky who provided the laboratory data used here to obtain the cosine error function, and to Paul Jindra for his help in revising the manuscript.

REFERENCES

Al-Jamal K., Ayyash S., Rasas M., Al-Aruri S. and Shaban N. (1987) Atmospheric turbidity in Kuwait. *Atmos. Environ* **21,** 1855–1859.

Barbaro S., Cannistraro G., Giaconia C., Orioli A. and Trapani S. (1989) An analysis of direct solar transmittance and atmospheric turbidity in the Mediterranean climatic belt. *Solar Wind Technol* **6,** 111–124.

Bird R. E. and Hulstrom R. L. (1982) Extensive modeled terrestrial solar spectral data sets with solar cell analysis. Rep. SERI/TR-215-1598. National Renewable Energy Lab., Golden, CO.

Braslau N. and Dave J. V. (1973) Effect of aerosols on the transfer of solar energy through realistic model atmospheres. *J. Appl. Meteorol* **12,** 601–619.

Cañada J., Pinazo J. M. and Bosca J. V. (1993) Determination of Angstrom's turbidity coefficient at Valencia. *Renew. Energy* **3,** 621–626.

Dogniaux R. and Doyen P. (1968) Analyse statistique du trouble atmosphérique à Uccle à partir d'observations radiométriques. Publ. A65. Institut Royal Météorologique, Uccle, Belgium.
Fox J. D. (1994) Calculated Ångström's turbidity coefficients for Fairbanks, Alaska. *J. Clim* **7,** 1506–1512.
Freund J. (1983) Aerosol optical depth in the Canadian Arctic. *Atmos. Ocean* **21,** 158–167.
Grenier J. C., de la Casinière A. and Cabot T. (1995) Atmospheric turbidity analyzed by means of standardized Linke's turbidity factor. *J. Appl. Meteorol* **34,** 1449–1458.
Gueymard C. (1989) A two-band model for the calculation of clear sky solar irradiance, illuminance, and photosynthetically active radiation at the Earth's surface. *Solar Energy* **43,** 253–265.
Gueymard C. (1994a) Analysis of monthly average atmospheric precipitable water and turbidity in Canada and Northern United States. *Solar Energy* **53,** 57–71.
Gueymard C. (1994b) Updated transmittance functions for use in fast spectral direct beam irradiance models. *Proc. Solar '94 Conf.*, San Jose, CA, American Solar Energy Society, pp. 355–360.
Gueymard C. (1995) SMARTS2, simple model of the atmospheric radiative transfer of sunshine: algorithms and performance assessment. Rep. FSEC-PF-270-95. Florida Solar Energy Center.
Gueymard C. (1998) Turbidity determination from broadband irradiance measurements: a detailed multicoefficient approach. *J. Appl. Meteorol* **37,** 414–435.
Gueymard C. and Garrison J. D. (1998) Critical evaluation of precipitable water and atmospheric turbidity in Canada using measured hourly solar irradiance. *Solar Energy* (in press).
Gueymard C. and Kambezidis H. D. (1997) Illuminance turbidity parameters and atmospheric extinction in the visible spectrum. *Q.J.R. Meteorol. Soc* **123,** 679–697.
Herman B. M., Browning R. S. and De Luisi J. J. (1975) Determination of the effective imaginary term of the complex refractive index of atmospheric dust by remote sensing: the diffuse-direct radiation method. *J. Atmos. Sci* **32,** 918–925.
IAMAP (1986) A preliminary cloudless standard atmosphere for radiation computation. Rep. WCP-112, WMO/TD-No. 24. World Meteorological Organization.
Jacovides C. P., Varotsos C., Kaltsounides N. A., Petrakis M. and Lalas D. P. (1994) Atmospheric turbidity parameters in the highly polluted site of Athens basin. *Renew. Energy* **4,** 465–470.
Jacovides C. P., Kaltsounides N. A., Giannourakos G. P. and Kallos G. B. (1995) Trends in attenuation coefficients in Athens, Greece, from 1954 to 1991. *J. Appl. Meteorol* **34,** 1459–1464.
Kambezidis H. D., Founda D. H. and Papanikolaou N. S. (1993) Linke and Unsworth–Monteith turbidity parameters in Athens. *Q.J.R. Meteorol. Soc* **119,** 367–374.
Katsoulis B. D. (1979) Turbidity of Greek sky. *Arch. Met. Geoph. Biokl* **B27,** 59–67.
King M. D. and Herman B. M. (1979) Determination of the ground albedo and the index of absorption of atmospheric particulates by remote sensing. Part 1: theory. *J. Atmos. Sci* **36,** 163–173.
Lacis A. A. and Hansen J. E. (1974) A parameterization for the absorption of solar radiation in the Earth's atmosphere. *J. Atmos. Sci* **31,** 118–133.
Latimer J. R. (1972) Radiation measurement. Tech. manual No. 2, International Field Year for the Great Lakes. National Research Council, Canada.
Louche A., Maurel M., Simonnot G., Peri G. and Iqbal M. (1987) Determination of Angström's turbidity coefficient from direct total solar irradiance measurements. *Solar Energy* **38,** 89–96.
Maxwell E. L., Marion W. F., Myers D. R., Rymes M. D. and Wilcox S. M. (1995) National Solar Radiation Data Base NSRDB Vol. 2. Rep. NREL/TP-463-5784. National Renewable Energy Lab., Golden, CO.
Michalsky J. J. and Dutton E. G. (1997) Optimal shortwave irradiance measurements for surface radiation balance studies. *Proc. Conf. Visual Air Quality, Aerosols, and Global Radiation Balance*, Air and Waste Management Association, Bartlett, NH, Vol. 2, pp. 791–799.
Michalsky J., Dutton E., Rubes M., Nelson D., Stoffel T., Wesely M., Splitt M. and DeLuisi J. (1998) Optimal measurement of surface shortwave irradiance using current instrumentation. *J. Atmos. Ocean. Technol.* (in press).
Michalsky J. J., Harrison L. C. and Berkheiser W. E. (1995) Cosine response characteristics of some radiometric and photometric sensors. *Solar Energy* **54,** 397–402.
Myers D. R., Emery K. A. and Stoffel T. L. (1989) Uncertainty estimates of global solar irradiance measurements used to evaluate PV device performance. *Solar Cells* **27,** 455–464.
Myers D. R. and Maxwell E. L. (1992) Hourly estimates of precipitable water for solar radiation models. *Proc. Solar '92 Conf.*, Cocoa Beach, FL, American Solar Energy Society, pp. 317–322.
O'Neill N. T., Royer A. and Miller J. R. (1989) Aerosol optical depth determination from ground based irradiance ratios. *Appl. Opt* **28,** 3092–3098.
Pinazo J. M., Cañada J. and Bosca J. V. (1995) A new method to determine Ångström's turbidity coefficient: its application for Valencia. *Solar Energy* **54,** 219–226.
Polavarapu R. J. (1978) Atmospheric turbidity over Canada. *J. Appl. Meteorol* **17,** 1368–1374.
Rawlins F. and Armstrong R. J. (1985) Recent measurements of broad-band turbidity in the United Kingdom. *Meteorol. Mag* **114,** 89–99.
Uboegbulam T. C. and Davies J. A. (1983) Turbidity in Eastern Canada. *J. Clim. Appl. Meteorol* **22,** 1384–1392.
Unsworth M. H. and Monteith J. L. (1972) Aerosol and solar radiation in Britain. *Q.J.R. Meteorol. Soc* **98,** 778–797.
Weber M. R. and Baker C. B. (1982) Comments on "the ratio of diffuse to direct solar irradiance (perpendicular to the sun's rays) with clear skies"—a conserved quantity throughout the day. *J. Appl. Meteorol* **21,** 883–886.
Wesely M. L. and Lipschutz R. C. (1976) An experimental study of the effects of aerosols on diffuse and direct solar radiation received during the summer near Chicago. *Atmos. Environ* **10,** 981–987.

APPENDIX

Parameterization of K_{db} as a function of atmospheric variables

The ratio $K_{db}=E_d/E_{bn}$ is evaluated with the SMARTS2 code for a large number of atmospheric conditions. The main variables are Ångström's β turbidity coefficient, the relative air mass, m, and precipitable water, w (in cm). The secondary variables are the station's altitude, z (in km), and total column ozone, u_o (in atm-cm). The assumptions include a continental/rural aerosol (IAMAP, 1986) and a Lambertian ground of albedo 0.15. The *predicted* ratio, K_{dbp}, can be parameterized by fitting this dataset to the following equation for fixed value of z (0 km or sea-level altitude) and of u_o (0.3434 atm-cm, from the U.S. Standard Atmosphere)

$$K_{dbp}=(a_0+a_1\beta+a_2\beta^2)/(1+a_3\beta^2). \qquad \text{(A1)}$$

This equation would lead to eqn (3) in the ideal case where the reference atmospheric conditions stated above are encountered. Because this is not the general case, K_{dbp} will not be used in the model and further treatment is necessary, as explained below.

The coefficients a_i ($i=0$–3) in eqn (A1) are themselves

Table A1. Coefficients c_{ijk} for eqn (A3)

i	j	$k=0$	$k=1$	$k=2$	$k=3$	$k=4$	$k=5$
$Z\leq 75^\circ$							
0	0	0.52117	1.006	−0.042873	0	28.975	0
	1	0.72229	0.89128	0	0	2.408	0
	2	0.082452	−.012294	0	0	−0.16285	0
	3	6.109	11.638	0	0	1.0197	0
	4	0.94808	0.70748	0	0	0.31929	0
1	0	1.6654	−0.2718	0.038852	0	0.097737	0
	1	26.736	0.6606	0.48453	0	0.5148	0
	2	9.9649	−0.90504	0.41026	0	0.78027	0
	3	14.975	−12.573	8.7377	−0.145	−0.77649	0.59698
	4	8.6269	4.2903	0.4548	0	2.8143	
2	0	0.97243	−1.202	0.42266	0.015911	−1.0995	0.43044
	1	3.7445	−0.19658	0	0	−0.4302	0.055777
	2	0.37223	0.2707	0	0	−0.41713	0.060103
	3	−28.048	88.745	0	0	7.1911	0
	4	−0.032032	0.69599	0	0	−0.19649	0.086467
3	0	19.971	−8.5353	2.184	−0.27494	6.1737	0
	1	−0.51917	0.89906	−0.22787	0	−2.6798	2.0256
	2	0	0	0	0	0	0
	3	0.25263	−0.055889	0.0028658	0	0.02773	0
	4	0	0	0	0	0	0
$Z>75^\circ$							
0	0	0.045782	7.2233E−5	0	0	0.1006	0
	1	0.48995	0.0034737	0	0	0.082245	0
	2	0.016878	0.24175	−0.0067237	0	2.324	0
	3	9.8712	1.2444	0	0	0.12268	0
	4	1.4222	0.095511	−0.0038319	0	0.033084	0
1	0	5.3519	3.693	−0.023403	0	5.4928	0
	1	81.626	56.225	−1.3526	0	5.6496	0
	2	14.512	0.26658	0.19442	0	1.2648	0
	3	18.472	24.599	−0.4754	0	1.8933	0
	4	4.2917	−0.30678	0.032554	0	0.087072	0
2	0	0.52476	0.22289	0.014775	0	0.11386	0
	1	5.6017	2.8016	0.15477	0	0.016973	0
	2	−3.8256	3.0417	−0.030759	0	0.13009	0
	3	9.7507	26.713	0.65182	0	2.6408	0
	4	1.3702	0.0049527	0	0	−0.082161	0.0077167
3	0	–	–	–	–	–	–
	1	−0.072783	0.02191	−0.0027096	0	0.13239	0
	2	0	0	0	0	0	0
	3	0.25263	−0.055889	0.0028658	0	0.02773	0
	4	0	0	0	0	0	0

parameterized as a function of w using

$$a_i=(b_{i0}+b_{i1}w+b_{i2}w^2)/(1+b_{i3}w+b_{i4}w^2). \quad \text{(A2)}$$

The coefficients b_{ij} ($j=0$–4) in eqn (A3) are functions of m and are obtained as

$$b_{ij}=(c_{ij0}+c_{ij1}m+c_{ij2}m^2+c_{ij3}m^3)/(1+{}_{cij4}m+c_{ij5}m^2) \quad \text{(A3)}$$

where the numerical values of the coefficients c_{ijk} ($k=0$–5) are given in Table A1. Note that these values are different for $Z\leq 75^\circ$ and $Z>75^\circ$. In the latter case, the only exception to eqn (A3) is for coefficient b_{30}:

$$b_{30}=(-0.078315+0.033421m+3.9515m^{-2.8})/(1-0.02397m). \quad \text{(A4)}$$

The relative air mass is calculated from the zenith angle, Z, using the following equation (Gueymard, 1995; Gueymard and Kambezidis, 1997)

$$m=1/[\cos Z+0.45665(Z^{0.07})(96.4836-Z)^{-1.697}]. \quad \text{(A5)}$$

The functional dependence of K_{db} on altitude and ozone are given by R and S. These functions "standardize" the *experimental* value of the diffuse-beam ratio, K_{dbx}, to zero altitude and u_o of 0.3434 atm-cm in order to match the conditions set for parameterizing β as a function of K_{db} (eqn (3)). Furthermore, a third factor, T, is introduced to account for the spectral mismatch between the wavelength range sensed by the pyrheliometer measuring E_{bn} (0.28–4 μm) and that sensed by the pyranometer measuring E_d or E (0.28–2.8 μm). These functions are parameterized as

$$R=(1-0.009z)(1+0.0041z-0.001179zm) \quad \text{(A6)}$$

$$S=(1.0148-0.043u_o)[0.98492+0.043907u_o+(0.004052-0.0118u_o)m] \quad \text{(A7)}$$

$$T=(0.98578+2.249w)/(1+2.26w). \quad \text{(A8)}$$

The standardized experimental value is

$$K_{db}=-\cos Z+(K_{dbx}+\cos Z)/(RST). \quad \text{(A9)}$$

This value of K_{db} needs to be inserted into eqn (3), along with the expressions for a_i from eqn (A2), so that eqn (3) can be finally solved for β. If the ground albedo value is different from its reference of 0.15, eqns (3)–(5) need to be solved iteratively.